Bainitic precipitation and its effect on the martensitic transformation in the Cu–Al–Ni–Mn–Ti shape-memory alloy

WENHUI ZOU‡, JIANIAN GUI‡, RENHUI WANG‡, CHENGHUAN TANG, MEIZHI XIANG, DI ZHANG
Department of Physics, Wuhan University, 43007 Wuhan, People's Republic of China, ‡ and also Beijing Laboratory of Electron Microscopy, Chinese Academy of Science, P.O. Box 2724, 10080 Beijing, People's Republic of China

WENHUA SUN
The Centre of Materials Science and Engineering, Dalian University of Technology, 116024 Dalian, People's Republic of China

DAZHI YANG
Department of Materials Science and Engineering, Dalian University of Technology, 116024 Dalian, People's Republic of China

Bainitic precipitation and its influence on the martensitic transformation in the Cu–11.9Al–5Ni–1.6Mn–1Ti (wt %) shape-memory alloy has been observed *in situ* using X-ray diffraction and transmission electron microscopy. Bainite was observed to be precipitated when the alloy was aged at 553–700 K. The orthorhombic distortion of the precipitated bainite decreased with increasing ageing temperature and time. The bainitic precipitation strongly decreased the martensitic transformation temperature, and changed the martensite from faulted $M18R_1$ type to twinned 2H type.

1. Introduction

Bainite formation is a highly controversial and widely debated subject ([1] and references cited therein). In copper-based Cu–Zn [2], Cu–Zn–Al [2–4], Cu–Zn–Au [5] and Cu–Al–Ni–Mn–Ti (CANTiM) [6, 7] alloys, the plate-shaped bainite has been found to be precipitated from the matrix during the isothermal heating in the mid-temperature range. Takesawa and Sato [2], Wu *et al.* [4], and Tadaki *et al.* [5] believed that bainitic transformation in these copper-based β-phase alloys with B2 or $L2_1$ type ordering, like in carbon steels, proceeds with characteristics of both martensitic and diffusion-controlled transformations. The study of bainitic precipitation is important, not only to clarify the transformation mechanism, but also from the view point of practical utilization of shape-memory alloys (SMAs), because preliminary investigation has shown that it strongly influences the martensitic transformation behaviour in the Cu–Zn–Al [3] and CANTiM [6] SMAs.

As a result of modification of Cu–13.5Al–4Ni (wt %) SMA, Cu–*x*Al–5Ni–2Mn–1Ti (wt %) system SMAs were developed [8], where $x = 11.8$–12.4. In CANTiM alloys, the substitution of aluminium by manganese and nickel suppresses the precipitation of brittle γ_2 phase while maintaining appropriate transition temperatures. Depending on the content, x, of aluminium, CANTiM alloys may be hypoeutectoid ($x < 12.7$) or hypereutectoid ($x > 12.7$). Obviously, a hypoeutectoid CANTiM alloy may precipitate bainite under certain conditions, as already observed by Itsumi *et al.* [6] and Zou *et al.* [7].

The present work aimed to study the process of the bainitic precipitation and its effect on the transition behaviour of the hypoeutectoid Cu–11.9Al–5Ni–1.6Mn–1Ti (wt %) SMA by *in situ* high-temperature X-ray diffraction and low-temperature transmission electron microscopy (TEM).

2. Experimental procedure

Plate specimens of Cu–11.9Al–5Ni–1.6Mn–Ti (wt %) CANTiM SMA were solid-solution treated at 1223 K for 20 min, and then either directly quenched into cold water (D Q) or step-quenched, i.e. quenched into an oil bath at 408 K for 30 min and then air-cooled. The martensitic and reverse transition temperatures M_s, M_f, A_s and A_f of the specimens, which are strongly dependent on the thermal treatment, were measured as $A_s \approx 455$ K, $A_f \approx 495$ K, $M_s \approx 440$ K and $M_f \approx 415$ K for the specimen directly quenched followed by thermal cycling. The surface layers of the treated specimens were removed by mechanical polishing followed by immersion in HCl–HNO_3–H_3PO_4 solution (volume ratio 1:4:5).

X-ray polycrystalline diffraction patterns were obtained by using a copper target and a graphite monochromator. In order to follow the continuous process

0022–2461

of the reverse transformation, the diffraction pattern from $2\theta = 50^\circ$ to $2\theta = 38^\circ$ was recorded repeatedly at a given heating rate.

TEM foils were prepared by double-jet electro-polishing from 3 mm diameter discs of 0.1 mm thickness using HNO_3–CH_3OH solution (volume ratio 1:2). TEM observation was carried out using a Philips CM-12 electron microscope equipped with a Gatan 613/633 double-tilting cooling holder operated at 120 kV.

3. Results

3.1. Bainitic precipitation

X-ray diffraction and TEM observation confirmed that the phases existing in the directly quenched specimen are $M18R_1$ type martensite and X-phase of $L2_1$ structure type with a composition of $(Cu, Ni)_2TiAl$ [7]. When this specimen was heated to 573 K for 2 h and then cooled to room temperature (RT), stabilized $N18R_1$ type martensite, retained parent phase of $L2_1$ structure type, X-phase and also bainite precipitation of disordered N9R structure-type, containing less alloying elements [7], were observed. When heated to 623 K for 2 h, at RT, basically the same constituent phases were observed except that the stabilized martensite in this case was disordered N9R type compared with the $N18R_1$ type in the at 573K heated specimen [7].

Fig. 1a–c show optical micrographs of the specimens directly quenched, DQ followed by heating at 573 K for 2 h, and DQ followed by heating at 623 K for 2 h, respectively. In Fig. 1(a) spear-like martensite and elliptical white X-phase particles can be clearly seen. Thin and broader bainite precipitates are observed in Fig. 1b and c, respectively. Moreover, the size of the X-phase particles increases with increasing heating temperature.

Fig. 2 shows a set of X-ray diffraction patterns of the DQ specimen. It can be seen from Fig. 2a that the DQ specimen consists of M18 R_1 martensite and X-phase at RT. By following the appearance of the $(2\,2\,0)_\beta$ peak of the parent phase when the temperature is increased continuously at the heating rate of 20 K min^{-1}, the reverse transition temperatures were found to be $A_s \approx 473$ K and $A_f \approx 520 \pm 20$ K. Fig. 2b shows the diffraction pattern when the specimen was heated to 553–573 K as indicated in the figure. This pattern reveals that all the $18R_1$ martensite has been reversely transformed into parent phase. When holding the specimen at 573 K for 11 min, diffraction peaks are observed nearly at the positions of $M18R_1$

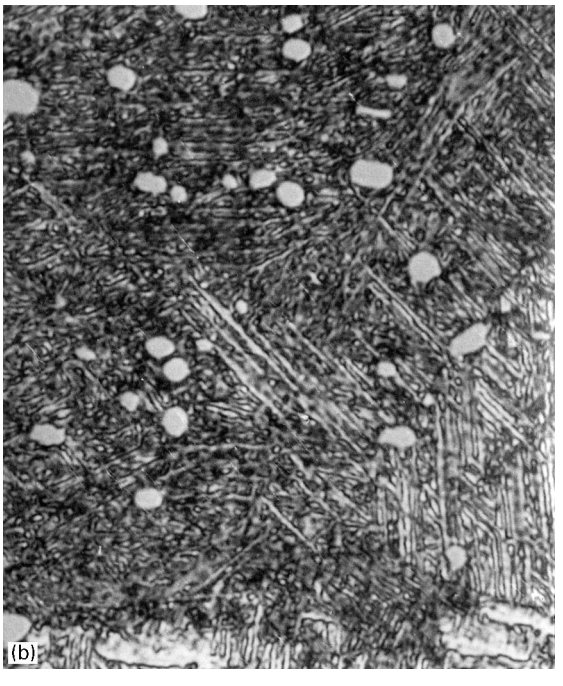

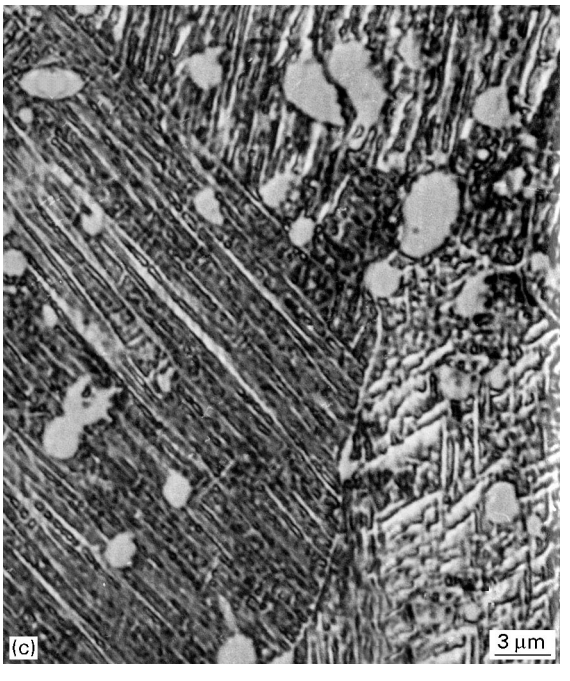

Figure 1 Optical micrographs of the CANTiM alloy photographed at RT: (a) directly-quenched; (b) DQ followed by heating at 573 K for 2 h; (c) DQ followed by heating at 623 K for 2 h.

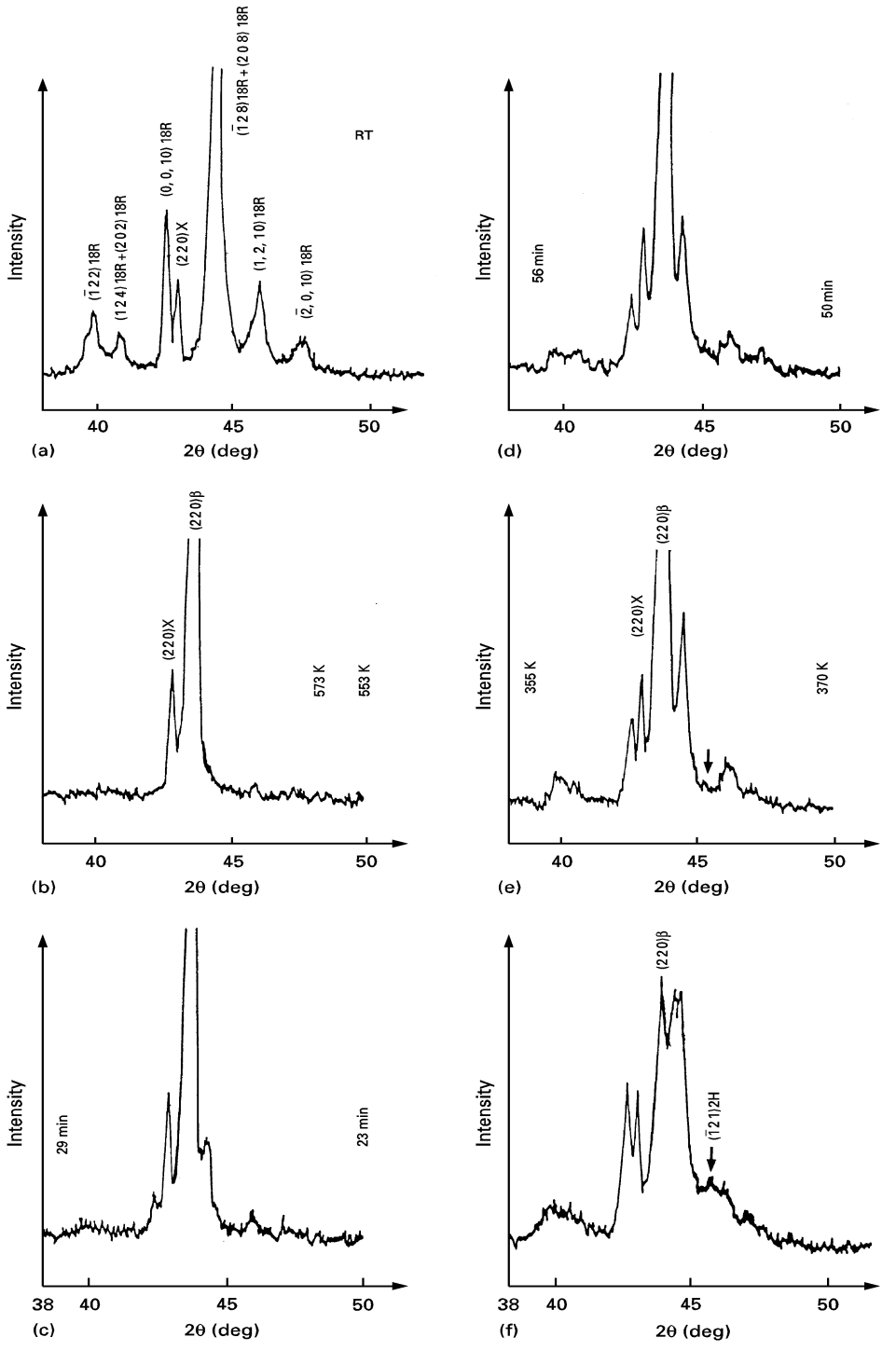

Figure 2 X-ray diffraction patterns during the heating and cooling processes of the directly quenched CANTiM alloy: (a) as-quenched specimen; (b) heated to 553–573 K at a heating rate of 20 K min^{-1}; (c) held for 23–29 min at 573 K; (d) held for 50–56 min at 573 K; (e) cooled to 370–355 K; (f) cooled at RT. In (c) and (d) the holding times are indicated, and in (b) and (e) the instantaneous temperatures are marked.

martensite peaks, but with smaller splitting of the line pairs $(\bar{1}\,2\,2)$–$(2\,0\,2)$ and $(1, 2, 10)$–$(\bar{2}, 0, 10)$. These peaks grew with increasing holding time; compare Fig. 2d with Fig. 2c. This fact obviously shows a bainitic precipitation. By comparing the integrated intensities of the bainite reflections after holding at 573 K for 2 h with those of the $18R_1$ martensite before heating (Fig. 2a), it can be concluded that nearly 38% parent phase was transformed into bainite. When the specimen was cooled, most of the retained parent phase transformed to martensite, compare the intensity of the $(2\,2\,0)_\beta$ peak at RT (Fig. 2f) with that at 362 K (Fig. 2e), and the M_s temperature was nearly 325 ± 30 K. The peak positions of the newly formed martensite are different from those of the bainite and hence cause broadening of some peaks in Fig. 2f.

Fig. 3 shows the bainitic precipitation when holding the DQ specimen at 623 K for 2 h. Other experimental conditions in this case were the same as those for Fig. 2. By comparing Fig. 3b and c, it can be seen that the incubation time of the bainitic precipitation at 623 K is less than 2 min, and the bainite reflection line pairs possess smaller splitting compared with those precipitated at 573 K. In this case, nearly 42% parent

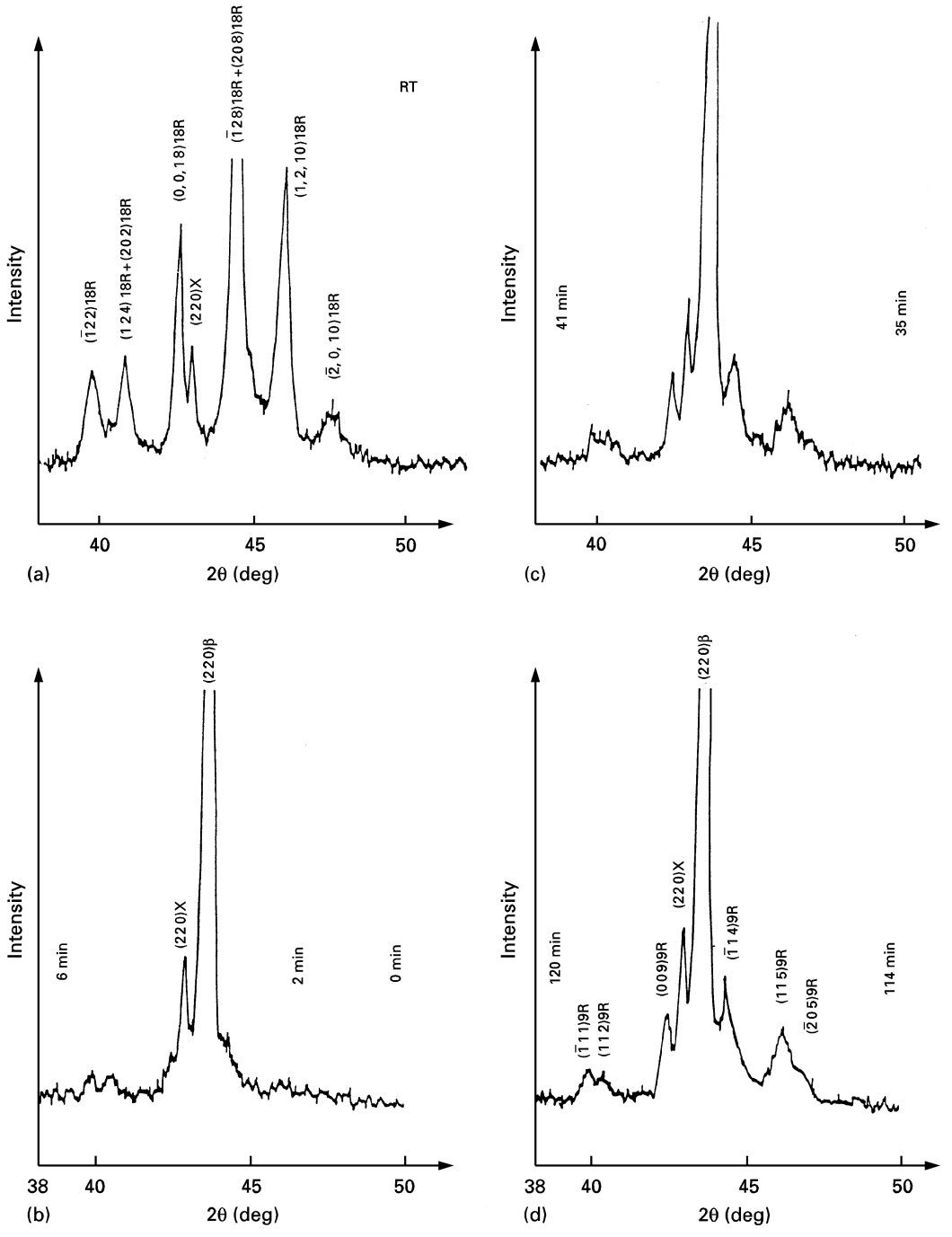

Figure 3 X-ray diffraction patterns showing the bainitic precipitation when holding the DQ CANTiM alloy at 623 K: (a) as-quenched specimen; (b) held for 0–6 min at 623 K; (c) held for 35–41 min at 623 K; (d) held for 114–120 min at 623 K.

phase was transformed into bainite and the M_s temperature was almost 300 K.

On holding the DQ specimen at 533 K for 2 h, no discernible bainite was found by X-ray diffraction, while little bainitic precipitation was observed on holding at 553 K.

Bainitic precipitation was also observed upon continuously heating the DQ and the step-quenched specimens by *in situ* X-ray diffraction experiments and it was found that bainite begins to precipitate when the temperature of the specimen reached 650 K at a heating rate of 20 or 10 K min^{-1}. This precipitation continued to about 700 K. When the temperature reached 850 K, all the reflection peaks belonging to bainite and stabilized martensite disappeared and transformed into those of equilibrium α and β parent phases. The line pair splitting of the bainite precipitated at 650–700 K are so small that both the line pairs $(\bar{1}\,2\,2)$–$(2\,0\,2)$ and $(1,2,10)$–$(\bar{2},0,10)$ coalesce, see Fig. 4c. Fig. 4a–c compare the diffraction patterns of the bainites precipitated at 573, 623 and 650–700 K, respectively, showing clearly that the orthorhombic distortion [9] of the bainite decreases with the increasing precipitation temperature. Table I lists the splitting values $\Delta 2\theta = 2\theta(h_1 k_1 l_1) - 2\theta(h_2 k_2 l_2)$ for line pairs $(\bar{1}\,2\,2)$–$(2\,0\,2)$, $(1,2,10)$–$(\bar{2},0,10)$ and $(0\,4\,0)$–$(3\,2\,0)$ and the lattice parameters a, b, c, β and φ for $M18R_1$ martensites and 9R bainites formed under different conditions where the lattice parameters are fitted from the 2θ values of the reflection peaks [9]. In Table I the

bond angle $\phi = 2\tan^{-1}[b/(2a)]$ is the angle between lines connecting the nearest neighbours in the basal plane of the martensite. The value of $\phi = 60^\circ$ corresponds to zero line-pair splitting and a larger ϕ indicates larger splitting and also larger orthorhombic distortion [9]. In order to simplify the description of Table I, we utilize the indices ($h\,k\,l$) and lattice parameters b and c related to the $18R_1$ structure type, irrespective of $18R_1$ or 9R structure type. Table I shows quantitatively that the splitting of the line pairs and also the orthorhombic distortion of the bainite, are smaller than those of the quenched martensite, and they decrease with increasing temperature at which the bainite precipitated.

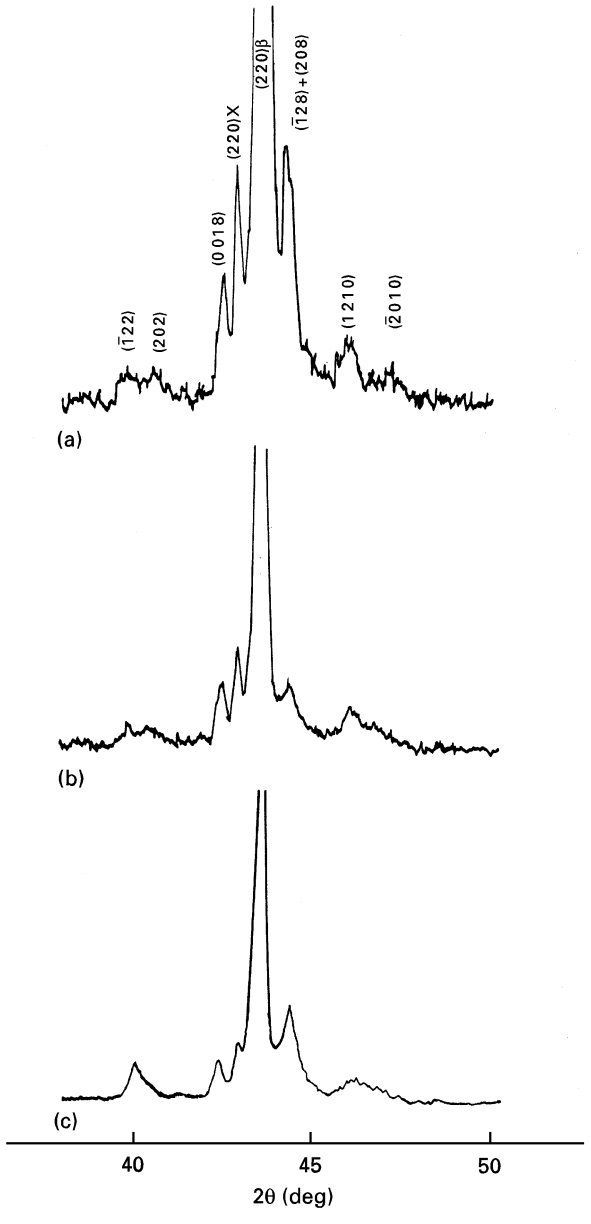

Figure 4 X-ray diffraction patterns showing the dependence of the orthorhombic distortion of the bainite upon precipitation temperature: (a) precipitated at 573 K from the DQ specimen; (b) precipitated at 623 K from the DQ specimen; (c) precipitated at 650–700 K from the step-quenched specimen.

3.2. Martensitic transformation

As described in Section 3.1, the M_s temperatures of the specimens held at 573 K and 623 K for 2 h are nearly $M_s \approx 325 \pm 30$ K and $M_s \approx 300$ K, respectively, much lower than that ($M_s \approx 440$ K) of the specimens which were not held at high temperature for a long time. Table II lists the M_s and M_f temperatures of the DQ specimens held at different temperatures for different times, showing the fact that the bainitic precipitation strongly decreases the martensitic transformation temperatures.

Fig. 5a shows a bright-field (BF) image of the DQ specimen after holding at 623 K for 2 h photographed at RT. Bainite plate and retained parent phase (regions A and B) can be clearly seen. By cooling the specimen in the electron microscope to 110 K, we observed that regions A and B transformed into twinned martensite (Fig. 5b). The selected-area electron diffraction pattern (EDP) shown in Fig. 5c reveals they are twinned 2H martensite with a $(1\,2\,1)_{2H}$ twin plane.

Fig. 6 displays a set of X-ray diffraction patterns taken from the DQ specimen held at 623 K for 2 h. When cooled to 295 K, the pattern is principally the same as Fig. 3d with a very strong $(2\,2\,0)_\beta$ peak of the parent phase. When cooled to 280, 263 and 77 K, and then the X-ray diffraction patterns recorded at 290 K, we obtain Fig. 6a–c, respectively. According to our previous work [10], we know that there are six peaks belonging to 2H martensite with the lattice parameters of $a = 0.441$ nm, $b = 0.527$ nm, $c = 0.423$ nm in the 2θ range of 38°–50°, i.e. $2\theta_{(1\,2\,0)2H} = 39.8^\circ$, $2\theta_{(2\,0\,0)2H} = 40.9^\circ$, $2\theta_{(0\,0\,2)2H} = 42.7^\circ$, $2\theta_{(2\,1\,0)2H} = 44.5^\circ$, $2\theta_{(\bar{1}\,2\,1)2H} = 45.4^\circ$ and $2\theta_{(2\,0\,1)2H} = 46.4^\circ$. Hence we can index the patterns shown in Fig. 6. From Fig. 6 it is obvious that with deeper cooling of the specimen, the quantity of retained parent phase decreases, and the quantity of the 2H martensite increases. This fact confirms further that the transformed martensite is 2H type with transition temperatures $M_f \leqslant 260$ K and $A_s \leqslant 290$ K.

Fig. 7 show an X-ray diffraction pattern of the DQ specimen subjected to the experiment shown in Fig. 2,

TABLE I Orthorhombic distortion of bainite precipitated at different temperatures compared with that of M18R_1 martensite

Specimen	Δ2θ(deg)			a (nm)	b (nm)	c (nm)	β (deg)	φ (deg)
	$(\bar{1}\,2\,2)$–$(2\,0\,2)$	$(1,2,10)$–$(\bar{2},0,10)$	$(0\,4\,0)$–$(3\,2\,0)$					
DQ martensite	1.0	1.62	2.30	0.4438	0.5300	3.829	88.75	61.68
408 K step-quenched martensite	0.87	1.45	2.10	0.4445	0.5289	3.827	88.78	61.50
Bainite precipitated at 573 K	0.67	0.85	1.10	0.4467	0.5242	3.826	89.38	60.80
Bainite precipitated at 623 K	0.5	0.72	0.8	0.4465	0.5217	3.828	89.59	60.59
Bainite precipitated at 650–700 K		Coalesced						

and then cooled to 283 K with higher angular resolution, where the main peaks are indexed. By comparing the peak intensities of the $(2\,2\,0)_\beta$ parent phase and those belonging to 2H martensite in Figs. 7, 2e and f, we found that the parent phase to 2H martensite transition began in the temperature range 355–295 K and was completed below 283 K.

TABLE II M_s and M_f temperatures of the DQ specimens held at different temperatures

Holding temp. (K)	Holding time (min)	M_s (K)	M_f (K)
537	0	440	420
553	20	420	370
533	120	390	360
623	20	380	330
553	120	370	> 300
573	120	325 ± 30	280
623	120	300	$\leqslant 260$

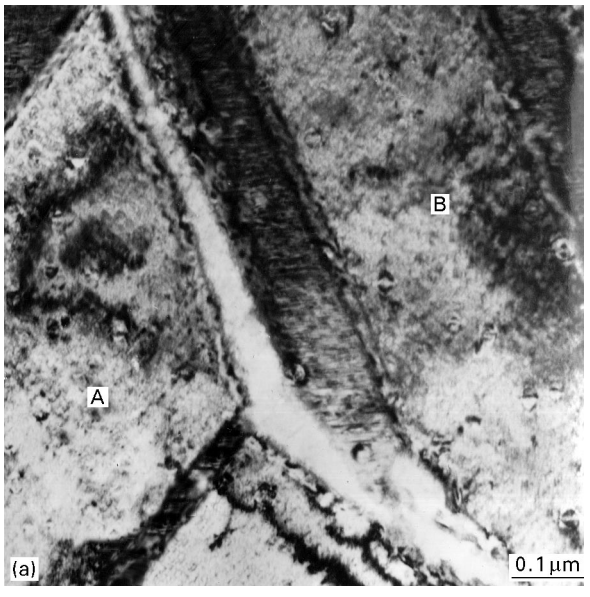

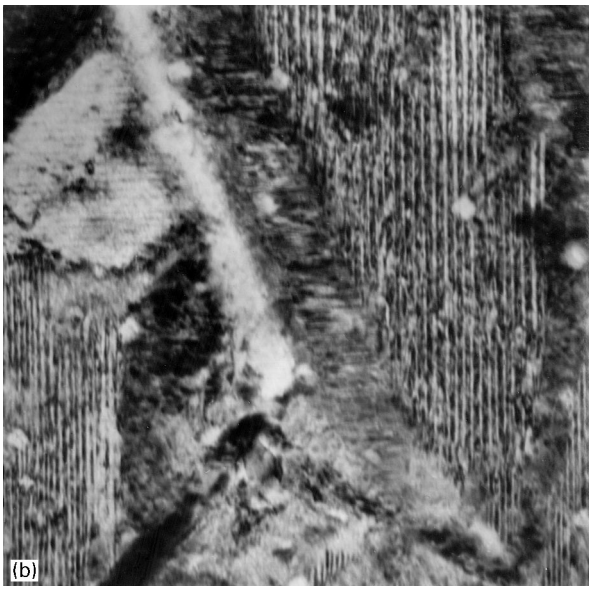

4. Discussion

It is well known that precipitation of γ_2 phase, which is rich in alloying elements, or bainite phase, which is poor in alloying elements, when holding a copper-based SMA at higher temperature, changes the content of the alloying elements in the parent phase [3, 10]. As summarized by Wu [11], the martensitic transformation temperature is very sensitive to small variations in alloy composition, and there is a linear empirical relationship for Cu–Al–Ni SMAs as follows:

$$M_s(\mathrm{K}) = 2293\text{–}45(\mathrm{wt\,\%\,Ni})\text{–}134(\mathrm{wt\,\%\,Al})$$

Moreover, Itsumi *et al.* [6] gave a similar relationship for the Cu–*x*Al–5Ni–2Mn–1Ti(wt %) CANTiM alloys: $A_s(\mathrm{K}) = 2013\text{–}135(\mathrm{wt\,\%\,Al})$. Hence it is not surprising that the bainitic precipitation strongly decreases both M_s and M_f temperatures, as listed in Table II. Usually there is bainite precipitation in Cu–Zn–Al SMAs [3] and γ_2 phase precipitation in Cu–Al–Ni SMAs [3, 10]. In CANTiM SMAs, either bainite or γ_2 phase may precipitate at higher temperature, depending on the aluminium content [6]. For the hypoeutectoid Cu–11.9Al–5Ni–1.6Mn–1Ti(wt %) CANTiM SMA studied in the present work, bainitic precipitation and a corresponding decrease of the transition temperatures were observed. In addition, a change of the martensite type from faulted $M18R_1$ to twinned 2H after bainitic precipitation was also noted, which is consistent with the existing phase diagram of Cu–Al binary alloys [12], the Cu–Al martensite has $18R_1$ type or 2H type structure when the aluminium content is lower or higher than 13 wt %.

Figure 5 Transmission electron micrographs showing the transformation from parent phase to twinned 2H martensite during cooling. The specimen had been held at 623 K for 2 h before this experiment. (a) BF image at RT where regions A and B were retained parent phase. (b) BF image at 110 K where the regions A and B transformed into twinned 2H matensite. (c) $[1\,0\,\bar{1}]_{2H}$ zone axis EDP take from the region B in (b) showing $(1\,2\,1)_{2H}$ twin relationship.

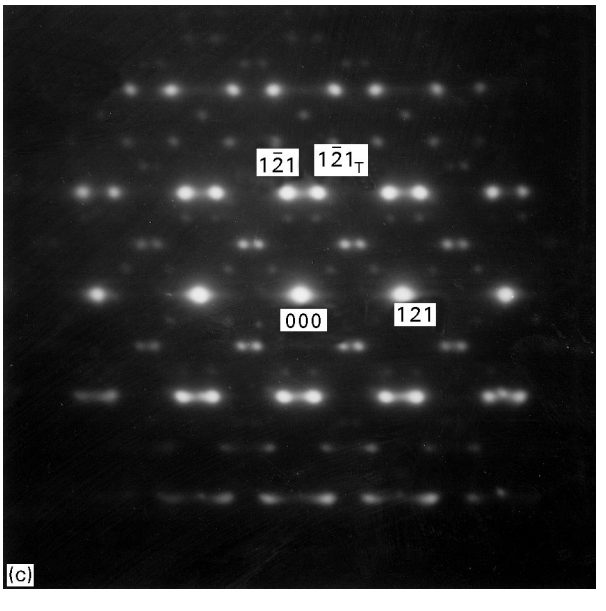

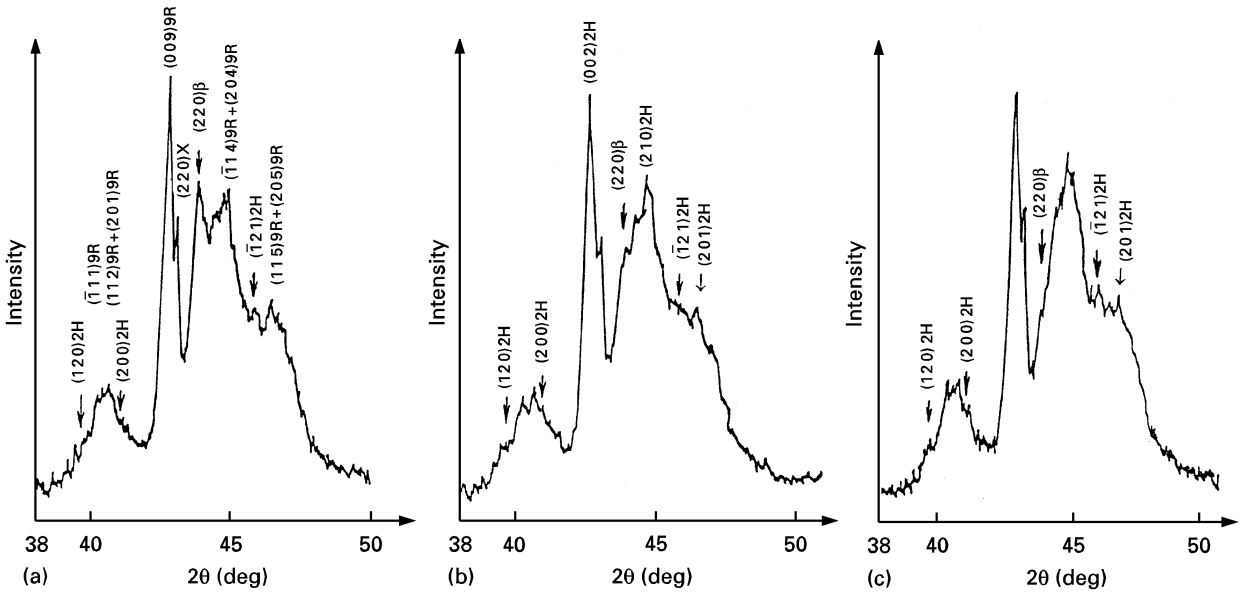

Figure 6 X-ray diffraction patterns of the DQ specimen held at 623 K for 2 h: (a) cooled at 280 K and then recorded at 290 K; (b) further cooled to 263 K and then recorded at 290 K; (c) further cooled to 77 K and then recorded at 290 K.

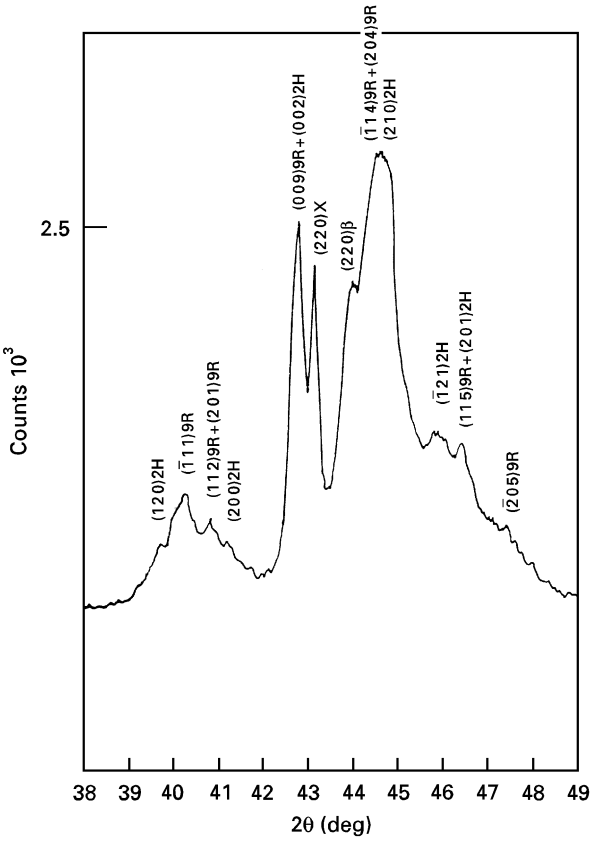

Figure 7 X-ray diffraction pattern of the DQ specimen held at 573 K for 2 h and then cooled to 283 K, possessing higher angular resolution by using a narrow (0.3 mm) receiving slit.

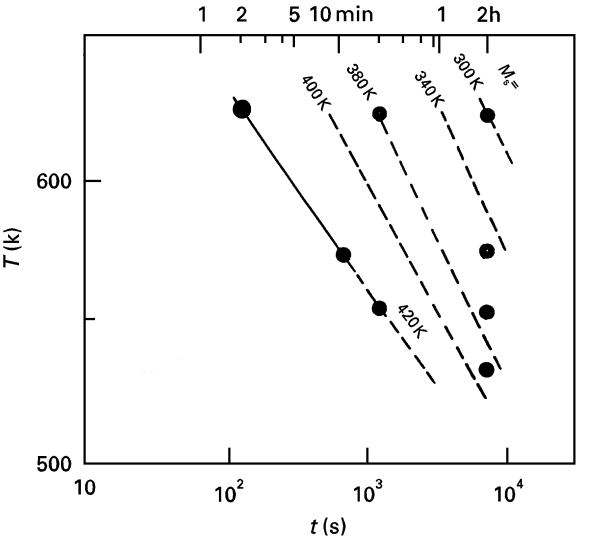

Figure 8 Bainite incubation curve and (– – –) M_s temperature chart on the coordinates of ageing temperature, T, and time, t, for the Cu–11.9Al–5Ni–1.6Mn–1Ti(wt %) SMA. (●) The experimental data. Temperatures marked in the chart indicate M_s temperatures.

One of the advantages of CANTiM SMA is the higher transition temperature [8], and hence it is very important whether this alloy has a lower tendency for bainitic precipitation. From the experimental results reported in Section 3.1 and the data listed in Table II, we can draw schematically a bainite incubation curve and an M_s temperature chart on the coordinates of ageing temperature, T, and time t, for the studied CANTiM SMA, as shown in Fig. 8. Fig. 8 shows that when the holding time is shorter than 2 h, then the CANTiM SMA can be held at a temperature lower than 520 K without discernible bainitic precipitation. Comparing the incubation curve measured in the present work with that for Cu–Zn–Al SMA [4, 13], we conclude that CANTiM SMA is more stable at high temperature than Cu–Zn–Al SMA.

The orthorhombic distortion of the bainite in CANTiM SMA as listed in Table I decreases and the structure type of the bainite varies towards N9R, corresponding to $\varphi = 60°$ and $\beta = 90°$ with increasing ageing temperature and time. This tendency is consistent with the bainite in Cu–Zn–Al SMA observed by

Wu *et al.* [13] who reported the variation sequence of $M18R_1 \rightarrow$ ordered $M9R \rightarrow$ disordered $N9R \rightarrow$ disordered fcc of the structure type of the α_1 bainites when the ageing temperature and time are increased.

Acknowledgement

This work was supported by the National Natural Science Foundation of China.

References

1. Proceedings of the Pacific Rim Conference on the Roles of Shear and Diffusion in the Formation of Plate-shaped Transformation Products, *Metall. Mater. Trans.* **25A** (1994) 1787, 2555.
2. K. TAKESAWA and S. SATO, *Mater. Trans. JIM* **32** (1991) 766.
3. N. F. KENNON, D. P. DUNNE and L. MIDDLETON, *Metall Trans.* **13A** (1982) 551.
4. M. H. WU, J. PERKINS and C. M. WAYMAN, *Acta Metall. Mater.* **37** (1989) 1821.
5. T. TADAKI, J. Q. CAI and K. SHIMIZU, *Mater. Trans. JIM* **32** (1991) 757.
6. Y. ITSUMI, Y. MIYAMOTO, T. TAKASHIMA, K. KAMEI and K. SUGIMOTO, *Mater. Sci. Forum* **56–58** (1990) 469.
7. W. H. ZOU, H. Y. PENG, R. WANG, J. GUI and D. Z. YANG, *Acta Metall. Mater.* **43** (1995) 3009.
8. K. SUGIMOTO, K. KAMEI and M. NAKANIWA, in "Engineering Aspects of Shape-Memory Alloys", edited by T. W. Duerig, K. N. Melton, D. Stöckel and C. M. Wayman (Butterworth, London, 1990) p. 89.
9. J. GUI, R. WANG and Y. ZHAO, *J. Appl. Crystallogr.* **21** (1988) 340.
10. Y. ZHANG, J. GUI, R. WANG, L. GAO, Y. WU and Y. TANG, *J. Phys. Condens. Matter* **5** (1993) 2719.
11. M. H. WU, in "Engineering Aspects of Shape-Memory Alloys", edited by T. W. Duerig, K. N. Melton, D. Stöckel and C. M. Wayman (Butterworth, London, 1990) p. 69.
12. P. R. SWANN and H. WARLIMOND, *Acta Metall* **11** (1963) 511.
13. M. H. WU, Y. HAMADA and C. M. WAYMAN, *Metall. Mater. Trans.* **25A** (1994) 2581.

Received 11 October 1995
and accepted 10 February 1997